Published in final edited form as:
Prostate. 2011 August 1; 71(11): 1198–1209. doi:10.1002/pros.21335.

Reactivation of Embryonic Nodal Signaling is Associated with Tumor Progression and Promotes the Growth of Prostate Cancer Cells

Mitchell G. Lawrence[1,*], **Naira V. Margaryan**[2], **Daniela Loessner**[1], **Angus Collins**[3], **Kris M. Kerr**[3], **Megan Turner**[3], **Elisabeth A. Seftor**[2], **Carson R. Stephens**[1], **John Lai**[1,**], **APC BioResource**[4], **Lynne-Marie Postovit**[5], **Judith A. Clements**[1,#], and **Mary J.C. Hendrix**[2,#]

[1] Australian Prostate Cancer Research Centre-Queensland and Institute of Health and Biomedical Innovation, Queensland University of Technology, Brisbane, Queensland, Australia, 4059

[2] Program in Cancer Biology and Epigenomics, Children's Memorial Research Center, Feinberg School of Medicine, Northwestern University, Chicago, Illinois, USA, 60614

[3] Sullivan Nicolaides Pathology, Brisbane, Queensland, Australia, 4068

[4] Australian Prostate Cancer BioResource

[5] Department of Anatomy and Cell Biology, Schulich School of Medicine and Dentistry, University of Western Ontario, London, Ontario, Canada, N6A 5C1

Abstract

Background—Nodal is a member of the Transforming Growth Factor β (TGFβ) superfamily that directs embryonic patterning and promotes the plasticity and tumorigenicity of tumor cells, but its role in the prostate is unknown. The goal of this study was to characterize the expression and function of Nodal in prostate cancer and determine whether, like other TGFβ ligands, it modulates androgen receptor (AR) activity.

Methods—Nodal expression was investigated using immunohistochemistry of tissue microarrays and Western blots of prostate cell lines. The functional role of Nodal was examined using Matrigel and soft agar growth assays. Cross-talk between Nodal and AR signaling was assessed with luciferase reporter assays and expression of endogenous androgen regulated genes.

Results—Significantly increased Nodal expression was observed in cancer compared with benign prostate specimens. Nodal was only expressed by DU145 and PC3 cells. All cell lines expressed Nodal's co-receptor, Cripto-1, but lacked Lefty, a critical negative regulator of Nodal signaling. Recombinant human Nodal triggered downstream Smad2 phosphorylation in DU145 and LNCaP cells, and stable transfection of pre-pro-Nodal enhanced the growth of LNCaP cells in Matrigel and soft agar. Finally, Nodal attenuated AR signaling, reducing the activity of a PSA promoter construct in luciferase assays and down-regulating the endogenous expression of androgen regulated genes.

[#]Correspondence: Mary J.C. Hendrix, Children's Memorial Research Center, Northwestern University, Feinberg School of Medicine, 2300 Children's Plaza, Box 222, Chicago, IL 60614-3394, m-hendrix@northwestern.edu and Judith A. Clements, Institute of Health and Biomedical Innovation, Queensland University of Technology, 60 Musk Avenue, Kelvin Grove, Queensland, 4059, j.clements@qut.edu.au.
[*]Current address: Department of Anatomy and Developmental Biology, Monash University, Clayton, Victoria, Australia, 3800.
[**]Current address: Department of Urology, Norris Cancer Center, University of Southern California, Los Angeles, California, USA, 90033.

Disclosure Statement: EAS, LMP and MJCH hold a patent on Nodal as a therapeutic target.

Conclusions—An aberrant Nodal signaling pathway is re-expressed and functionally active in prostate cancer cells.

Keywords

Nodal; Cripto-1; Lefty; Prostate Cancer; Androgen Receptor

Introduction

Cancer has been described as a “caricature” of development because it exaggerates some aspects and under-represents others (1). This holds true for prostate cancer (2). Microscopically, prostate cancer is characterized by increasingly dedifferentiated tumor cells, as measured with the Gleason grading system. On the molecular level, the gene expression profile of human prostate cancer resembles that of budding mouse urogenital epithelium (3). Similarly, prostate tumors in PTEN knockout and c-myc over-expressing mice reactivate the gene expression signature of branching morphogenesis within the mouse fetal prostate (4). Unlike some tumors, prostate cancer invokes a tissue-specific, rather than generic, developmental gene expression profile (3–5). The lineage-specific interpretation of developmental cues may be due to cross-talk with androgen receptor signaling, since it is essential for fetal prostate development and adult prostate cancer (2). Overall, these observations suggest that developmental signaling molecules may be important mediators of prostate cancer progression.

The Transforming Growth Factor β (TGFβ) superfamily, which includes bone morphogenetic proteins (BMPs), activins and TGFβs, is a prominent example of the signaling pathways that regulate development and cancer. Components of this family are differentially expressed during key stages of prostate development, including budding, branching morphogenesis and pubertal growth (3,4,6,7). A caricature of normal TGFβ signaling also promotes prostate cancer progression once the tumor cells become responsive to the pro-migratory, but not anti-proliferative, effects of this pathway (8,9). Importantly, extensive cross-talk with the AR pathway is likely to modulate the functions of the TGFβ superfamily in the prostate (9).

A member of the TGFβ superfamily that has so far been overlooked in prostate cancer is Nodal, which is crucial for embryogenesis and has an emerging role in tissue morphogenesis (10–12). Nodal is already expressed by the blastocyst stage of mammalian development (13), so it is secreted by human embryonic stem cells (hESCs) where it maintains pluripotency and inhibits differentiation (14,15). After embryo implantation, the epiblast continues to express Nodal, which subsequently stimulates endoderm and mesoderm formation and left-right axis specification (11). Later, Nodal induces embryonic heart formation and has a role in development of the breast and pancreas (10,12,16). Of particular note to this study, Nodal has recently been shown to be re-expressed in breast and endometrial cancer, melanoma and glioma (17–20).

Nodal, like activins, binds as a dimer to type I (ALK4/ActRIB) and type II serine-threonine kinase receptors (ActRIIA or ActRIIB) and triggers downstream phosphorylation of Smad2 and Smad3 (21). These receptor-regulated Smads then associate with Smad4, translocate to the nucleus, and synergistically activate gene expression with a range of transcription factors. Nodal and activin B, but not activin A, may also signal through Alk7 (22). Nodal is unique among the TGFβ superfamily, because it requires co-receptors from the EGF-CFC family to potentiate activin receptor signaling (21). Humans have two EGF-CFC receptors, Cripto-1 and Cryptic, which have distinct expression profiles. Notably, Cripto-1 is expressed in a wide range of malignancies and has Nodal-independent functions, including activation

of the PI3K/Akt, Src and ras/raf/MAPK pathways (23). In embryos, Nodal signaling is also tightly regulated by inhibitors, including Lefty A and B, Cerberus and TMEFF1 (21). Tumor cells, however, tend to lack these inhibitors, which means that Nodal signaling is dysregulated (18,20).

Reactivation of Nodal signaling may have important functional consequences for prostate cancer progression. Yet, unlike other members of the TGFβ superfamily, little is known about Nodal in prostate cancer. Therefore, the goal of this study was to characterize the expression of the Nodal pathway in prostate cancer and investigate the functional effects of Nodal, including its impact on AR activity.

Materials and Methods

Immunohistochemistry

Tissue microarrays of prostate specimens from radical prostatectomies were obtained from the Northwestern University Prostate SPORE and The Australian Prostate Cancer BioResource and used with Queensland University of Technology ethics approval. Cores spanned benign tissue to Gleason grade 9 prostate cancer and were graded by a team of urological pathologists. Nodal staining was performed as previously outlined (18,19) using a goat anti-Nodal antibody (R&D Systems, Minneapolis, MN) and normal goat IgG control (Jackson ImmunoResearch Laboratories, West Grove, PA) with 3,3′-diaminobenzadine (DAB) as the chromogen and Mayer's hematoxylin counterstaining. Nodal staining was scored as negative (0), weak (1), moderate (2) or strong (3) by three investigators. Specimens were also co-stained for alpha-methylacyl-CoA racemase (AMACR), p63, and high molecular weight cytokeratins (Dako, Carpinteria, CA) to discriminate between benign and malignant regions (24). AMACR was visualized with 3-amino-9-ethylcarbazole (AEC), while p63 and high molecular weight cytokeratins were detected with DAB.

Cell Culture

LNCaP, PC-3, 22Rv1 and DU145 human prostate cells were cultured in RPMI-1640 supplemented with 10% fetal calf serum (FCS), 50 U/mL Penicillin G, and 50 μg/mL Streptomycin (Invitrogen, Carlsbad, CA). The MDA-PCa-2b human prostate cancer cell line was grown in BRFF-HPC1 media with 20% FCS (AthenaES, Baltimore, MD). H9 hESCs were maintained in 80% Dulbecco's modified Eagle's medium-F12 and 20% knockout serum replacer with 1% nonessential amino acids, 1 mM L-Glutamine, and 4 ng/ml basic fibroblast growth factor (Invitrogen) on a feeder layer of irradiated mouse embryonic fibroblasts (MEFs; strain CF-1; American Type Culture Collection). MEL1 hESC lysates were a generous gift from the Australian Stem Cell Centre StemCore.

Reverse Transcription PCR and Real-Time RT-PCR

Total RNA was extracted with TRIzol (Invitrogen), treated with DNase I, and reverse transcribed with the SuperScript III First-Strand Synthesis System (Invitrogen). The reverse transcriptase (RT) was omitted from some reactions to generate minus RT controls. Cripto-1, Lefty A/B, Cerberus and TMEFF1 were amplified with Platinum *Taq* polymerase (Invitrogen) using GAPDH as a control. Products were separated using agarose gel electrophoresis, stained with ethidium bromide and visualized under UV light. Real-time RT-PCR was performed on an ABI7300 or ABI7900 thermocycler (Applied Biosystems, Foster City, CA) using a Taqman primer/probe set for Nodal (Hs00250630_s1; Applied Biosystems). KLK2, PSA, TMPRSS2, NKX3.1 and GAPDH were amplified with gene specific primers and SYBR Green Master Mix (Applied Biosystems). KLK2 and PSA expression was normalized to GAPDH using the delta-delta Ct method, while NKX3.1 and TMPRSS2 levels were normalized to GAPDH using arbitrary standard curves of purified

PCR products. All primer sequences are listed in Table 1. The annealing temperature was set at 60 oC for all reactions.

Immunoprecipitation and Western Blotting

Cell lystates were prepared in RIPA buffer and protein concentrations were measured using the bicinchoninic acid assay (Sigma Aldrich, Castle Hill, NSW, Australia). For Nodal immunoprecipitation, 1 mg of lystate was precleared and incubated overnight at 4°C with 2 μg of either rabbit anti-human Nodal (Epitomics, Burlingame, CA) or goat anti-mouse Nodal (R&D Systems) antibodies. Samples were then incubated with protein G agarose (Roche Diagnostics, Castle Hill, NSW, Australia) for 1 hr at 4 °C and centrifuged at 2500 x g for 5 min. Supernatants were retained and later probed for GAPDH. Pellets were washed and then boiled in Laemmli buffer. Immunocomplexes and whole cell lysates were separated using SDS polyacrylamide gel electrophoresis. Membranes were probed with Nodal (mouse: Abnova, Taipei City, Taiwan), Cripto-1 (mouse: Rockland Immunochemicals, Gilbertsville, PA), phosphorylated Smad2, total Smad2/3 (Cell Signaling Technology), FLAG (Sigma Aldrich) or GAPDH (Abcam, Cambridge, MA) primary antibodies and donkey-anti-mouse-800 (Rockland Immunochemicals) or goat-anti-rabbit-680 (Invitrogen) fluorescent secondary antibodies. Blots were visualized using a LI-COR Odyssey scanner (LI-COR Biotechnology, Lincoln, NE).

Recombinant Nodal Treatments

DU145 and LNCaP cells were grown to 50% confluence and cultured overnight in serum-free RPMI 1640. For time course experiments, DU145 cells were treated with 1 μg/mL recombinant mature human Nodal (R&D Systems) for 5 min to 1 hr. Recombinant human TGFβ (1 ng/mL, R&D Systems) was used as a positive control. For dose response experiments, DU145 cells were treated with 10–1000 ng/mL Nodal and 10 μM SB431542 (Sigma Aldrich), an Alk 4/5/7 inhibitor, or DMSO vehicle control. LNCaP cells were treated with 500 ng/mL Nodal for 6 hrs with fresh recombinant Nodal added every 2 hrs.

Generation of Polyclonal Stable Cells

Human pre-pro-Nodal was amplified from H9 hESC cDNA (Fwd: 5′ TCCCTCCAGGATGTCTCGAGAGGCACCCAC 3′, Rev: 5′ TTCAGGATCCGCCAGCCCACCATGCACGCC 3′) and cloned into the pcDNA3.1 Flag-His vector using BamHI and XhoI restriction endonuclease sites (Invitrogen) so that the epitope tag was at the C-terminus of Nodal. Inserts were sequenced at the Australian Genome Research Facility, Brisbane, Australia, which confirmed the verity of the cloned product. Early passage LNCaP cells were transfected with 10 μg of Nodal or vector only plasmid DNA using Lipofectamine 2000 (Invitrogen). Geneticin (Invitrogen) was added for selection (800 μg/mL) and maintenance (400 μg/mL) of stable transfectants.

Matrigel and Soft Agar Growth Assays

Stably-transfected LNCaP cells were seeded into cylindrical constructs of growth factor-reduced Matrigel (BD Biosciences, San Jose, CA) using a previously described technique (28). Briefly, cells were harvested with 0.48 mM EDTA and resuspended in undiluted Matrigel at 3.5×10^5 cells/mL. Cylindrical Matrigel constructs were formed by pipetting 20 μL of cell suspension between two microscope slides treated with SigmaCote (Sigma Aldrich) and separated by 1 mm plastic spacers. The slides were clamped together and the Matrigel was polymerized at 37 °C for 30 min. The disks were dislodged using a scalpel blade, placed in media, collected after 1, 3, 6, 9 and 12 days in culture and frozen. Subsequently, Matrigel constructs were digested overnight at 65 °C with 0.5 mg/mL proteinase K in phosphate-buffered EDTA and the DNA content was measured using the

CyQUANT cell proliferation assay kit (Invitrogen) according to the manufacturer's instructions. The experiment was performed 3 times with 3–5 constructs for each time point. Anchorage-independent growth was tested in 6-well plates coated with RPMI 1640 containing 10% FCS and 0.5% agar. Stably transfected LNCaP cells were seeded at 5×10^3 cells/well in media containing 0.35% agarose. Once macroscopic colonies formed, they were stained with 0.001% crystal violet and counted. The percentage of clonogenic cells was calculated by dividing the number of colonies by the number of cells seeded. The assay was performed 3 times with 6 replicates per experiment. Phase contrast images were taken using a brightfield microscope (Eclipse TE2000-U, Nikon; LaborLux S, Leitz) with 10x and 40x air objectives.

Luciferase Assays

For luciferase assays, 6×10^4 LNCaP cells/well were seeded in 24-well plates and cultured in phenol red-free RPMI 1640 medium containing 10% charcoal-stripped serum (HyClone, Denver, CO) for 72 hrs. Each well was transfected with 300 ng of a pGL3Basic luciferase construct containing 5.8 kilobases of the PSA promoter (29), 300 ng of Renilla, 10–250 ng of Nodal pcDNA3.1 Flag-His and various concentrations of empty pcDNA3.1 Flag-His vector to ensure equimolar amounts of total plasmid DNA. After 6 hrs, cells were treated with 1 nM R1881 (Perkin Elmer, Boston, MA) or ethanol vehicle control for 24 hrs before luciferase activity was quantified using the Dual-Luciferase Reporter Assay System (Promega, Annandale, Australia) on a PolarStar plate reader (BMG, Labtech, Offenburg, Germany). Three experiments were performed in triplicate.

Data Analysis

Statistical analyses were conducted with R (www.r-project.org). *P*-values less than 0.05 were considered to be significant and are indicated as * for $P<0.05$, ** for $P<0.01$, *** and $P<0.001$. All data are shown as means of experimental replicates with error bars representing the standard error of the mean (SEM).

Results

Nodal Expression Increases Prostate Cancer Progression

To determine whether Nodal is dysregulated in prostate cancer, tissue microarrays comprising 506 cores were stained using the same procedure as previous studies with breast cancer and melanoma specimens (18,19). Little or no Nodal immunoreactivity was observed in normal glands, while strong cytoplasmic staining of epithelial cells was detected in Gleason patterns 3–5 prostate cancer (Figure 1A). There was negligible staining with the isotype primary antibody control. We next examined Nodal expression in cores that had adjacent cancer and benign regions based on staining with a cocktail of AMACR, p63 and HMW keratin antibodies (Figure 1B&C). Nodal staining was stronger in the malignant versus benign glands of 67 % (35 of 52) of these cores. There was no difference in the intensity of Nodal staining in 33% of the cores (17 of 52), most of which had no staining or just background staining. No instances of higher Nodal expression in benign versus malignant glands were observed. To further investigate changes in Nodal expression with prostate cancer progression, the intensity of Nodal staining was compared to Gleason score (Figure 1D). There was a significant association between Nodal intensity and prostate cancer when benign cores were compared to all tumor specimens ($P=0.4\times10^{-21}$). There was no correlation between Nodal staining and individual Gleason scores; however, there was a significant difference in Nodal intensity between low grade (Gleason score ≤6) and high grade (Gleason score ≥ 7) prostate cancer ($P=0.9\times10^{-4}$). These data demonstrate that there is increased Nodal expression with prostate cancer progression.

Nodal and Cripto-1 are Expressed in Prostate Cancer Cell Lines

To identify appropriate models to study the function of Nodal in prostate cancer, the expression of key members of the Nodal signaling pathway was characterized in LNCaP, 22Rv1, PC3, DU145 and MDA-PCa-2b cells. Real-time PCR confirmed that all prostate cancer cell lines express Nodal mRNA, with the highest levels detected in PC3 and DU145 cells (Figure 2A). H9 hESCs were used as a positive control because they express high levels of Nodal, indeed 50- to 100-fold more than the prostate cancer cell lines. Minus RT controls were included for all samples since the Nodal primer-probe set does not span an intron (data not shown). Nodal protein expression was detected using immunoprecipitation because it was more sensitive and specific than Western blots with available Nodal antibodies. LNCaP cells stably transfected with Nodal were used as a positive control. Endogenous Nodal was consistently detected in DU145 cells using different combinations of Nodal antibodies (Figure 2B). The 42 kDa band for endogenous and stably transfected Nodal corresponds to the glycosylated pre-pro-form of the protein (30). Low levels of Nodal were occasionally observed in PC3 cells (data not shown). Nodal was not detected in LNCaP, 22Rv1 and MDA-PCa-2b cells, which expressed lower levels of Nodal mRNA.

Like Nodal, its co-receptor Cripto-1 was expressed at the mRNA levels in all prostate cancer cell lines (Figure 2C). Although the PCR primers span intron 3 of the Cripto-1 gene, minus RT controls were necessary to exclude genomic DNA contamination and amplification of Cripto retropseudogenes, which lack introns (31). Unlike Nodal, Cripto-1 protein was also detected in all prostate cancer cell lines (Figure 2D). Consistent with the extensive post-translational modification of Cripto-1 (32,33), two bands of approximately 17 and 25 kDa were observed in prostate cancer cell lines. An additional 19kDa band was also detected for MEL1 hESCs. The expression of the other Nodal co-receptor, Cryptic, was also examined; however, it was not detected using RT-PCR (data not shown). The expression of both Nodal and Cripto-1 in DU145 cells implies that the pathway may be active in this cell line. Lefty A/B, Cerberus and TMEFF1, which inhibit Nodal signaling in embryos, were all detected in hESCs using RT-PCR (Figure 2E). In contrast, little or no expression of these inhibitors was observed in prostate cancer cell lines. There were barely detectable bands for Lefty A/B in MDA-PCa-2b cells and TMEFF1 in 22Rv1 and DU145 cells. These results suggested that prostate cancer cells may engage in Nodal signaling in an unregulated manner with little to no inhibition by Lefty A/B, Cerberus or TMEFF1.

Prostate Cancer Cells are Responsive to Nodal

Prostate cancer cells were treated with recombinant mature Nodal (rNodal) to confirm that the Nodal pathway is functionally active. DU145 cells, which express Nodal and Cripto-1, and LNCaP cells, which only express Cripto-1, were used. In time course experiments treated with 1 μg/mL rNodal, increased pSmad2 levels were detected after 30 min, with a maximal significant response after 60 min (Figure 3A). Recombinant TGFβ1 was used as a positive control and was more potent than Nodal, stimulating greater Smad2 phosphorylation at a concentration of 1 ng/mL. Therefore, dose response experiments were used to test lower concentrations of rNodal. Small increases in pSmad2 were observed with 10 and 100 ng/mL rNodal, whereas 500 and 1000 ng/mL resulted in marked phosphorylation (Figure 3A). The Alk4/5/7 inhibitor SB431542 abolished this Nodal-induced Smad2 phosphorylation. This confirms that Smad2 phosphorylation was specific and not due to low affinity binding of Nodal to non-physiological receptors. A significant increase in pSmad2 was observed when LNCaP cells were treated with 500 ng/mL rNodal for 6 hrs (Figure 3B). Collectively, these experiments demonstrate that prostate cancer cells are indeed responsive to Nodal.

Nodal Enhances the Growth of Prostate Cancer Cells

To investigate the functional consequences of Nodal signaling, LNCaP cells were stably transfected with a Nodal expression construct (LNCaP-Nodal) or the empty vector control (LNCaP-Vector). The expression of Flag-tagged Nodal in LNCaP-Nodal but not LNCaP-Vector cells was verified by Western blot (Figure 4A). Their growth was then measured over 12 days in three-dimensional Matrigel constructs. There was a trend of increased growth of LNCaP-Nodal compared to LNCaP-Vector cells by day 9, which reached significance at day 12 (Figure 4B). Indeed, there was a 35-fold increase in LNCaP-Nodal cells, but only 23-fold increase in LNCaP-Vector cells over the course of this assay. Confirming these data, phase contrast images showed that LNCaP-Nodal cells formed larger clusters in Matrigel than LNCaP-Vector cells (Figure 4C). Using soft agar assays, the anchorage-independent growth of these cells was also examined. A significantly higher proportion of LNCaP-Nodal cells were able to form colonies compared to LNCaP-Vector cells (Figure 4D&E). These results demonstrate that Nodal promotes the growth of prostate cancer cells in both extracellular matrix-rich and anchorage-independent conditions.

Nodal Reduces Androgen Receptor Activity

Given that AR signaling is integral to the survival of prostate cancer and several members of the TGFβ superfamily modulate this activity, we examined the effect of Nodal on androgen responsiveness. LNCaP cells were co-transfected with a PSA luciferase reporter and the Nodal construct or vector control and then treated for 24 hrs with 1 nM of R1881, which is a synthetic, non-metabolizable androgen. In the absence of Nodal, there was a 6-fold increase in PSA reporter activity (Figure 5A). Increasing amounts of the Nodal construct significantly attenuated PSA luciferase activity in R1881-treated cells. Endogenous PSA expression was also down-regulated in stably transfected LNCaP-Nodal versus LNCaP-Vector cells (Figure 5B). Other prototypical androgen regulated genes, including KLK2, TMPRSS2 and NKX3.1, were also significantly down-regulated. These results demonstrate that Nodal, like some other members of the TGFβ superfamily, antagonizes AR signaling in prostate cancer cells.

Conclusions

During prostate cancer progression, developmental signaling pathways are re-activated and exploited by tumor cells with an increasingly dedifferentiated phenotype. In this study, we demonstrated that Nodal, which is essential for normal embryogenesis, is re-expressed in prostate cancer tissue specimens and cell lines. Importantly, Nodal is also functionally active, inducing downstream Smad2 phosphorylation and increased growth of prostate cancer cells. Additionally, it modulates AR signaling, a key pathway in prostate cancer progression.

Previous studies have shown that Nodal is up-regulated in breast and endometrial cancer, melanoma and glioma patient specimens and that there is increased Cripto-1 expression in cancers of the breast, colon, lung, ovary, endometrium, cervix, gall bladder, pancreas and stomach (17–20,32). Until now, data on the expression profile of the Nodal signaling pathway in prostate cancer has been limited to Cripto-1. For example, Cripto-1 mRNA has been detected in CD133 positive primary prostate epithelial cells as well as LNCaP and PC3 cells grown in soft agar (34,35). Notably, it has been shown that Cripto-1 over-expression increased the clonogenicity of PC3 cells, whereas Cripto-1 blocking antibodies inhibited the growth of LNCaP, PC-3 and DU145 cells *in vitro* (36,37). These data suggested that Nodal signaling may be important for the growth and survival of prostate cancer cells. Therefore, we further investigated the expression of key components of the Nodal signaling pathway in prostate cancer. Using immunohistochemistry we found that there was a significant increase

in Nodal staining in prostate cancer versus benign patient specimens. Indeed, 88% of benign cores exhibited low or no Nodal staining, whereas 61% of malignant samples had moderate to high staining. Nodal protein expression was also detected in the DU145 prostate cancer cell line. Cripto-1 mRNA and protein were detected in all cell lines used. The Cripto-1 primers and antibodies may also detect Cripto-3, a less well characterized Cripto homolog; however, no amplification was observed using Cripto-3-specific PCR primers (data not shown) (38). Previous studies have confirmed the expression of activin type II receptors and Smad2/3 (39,40). In contrast to Nodal and Cripto-1, little or no Lefty and Cerberus mRNA were expressed in prostate cell lines. Low levels of TMEFF1 were detected in 22Rv1 and DU145 cells, similar to a previous study with C8161 melanoma cells (41). Collectively, these results suggest that the Nodal signaling pathway is reactivated in prostate cancer in an unregulated manner due to the absence of notable Nodal inhibitors.

Prostate cancer cells not only express components of the Nodal signaling pathway, they are also responsive to Nodal signaling. Recombinant Nodal triggered Smad2 phosphorylation in both Nodal expressing DU145 cells, as well as LNCaP cells, which lack Nodal expression. These results imply that Nodal is able to act in *trans* on prostate cancer cells expressing Cripto-1. A soluble form of Cripto-1 lacking its GPI anchor can also activate non-cell autonomous Nodal signaling in embryos and cancer cell lines (33,42,43). Significantly, there are increased levels of soluble Cripto-1 in the sera of breast and colon cancer patients (44). Therefore, a subpopulation of cancer cells producing Nodal and Cripto-1 could theoretically signal to adjacent cells as long as they express ActRIIA/B and Alk4/7. This would be exacerbated by the lack of Lefty and Cerberus feedback inhibition.

Higher concentrations of Nodal were needed to induce Smad2 phosphorylation in DU145 cells compared with TGFβ1, which binds to TGFβ receptor I (TGFβRI/Alk5) and TGFβRII (45). LNCaP cells were not treated with TGFβ1, because they do not express TGFβRI and TGFβRII due to promoter methylation (46,47). Our results are consistent with other studies showing that Nodal signaling is less potent and efficient than TGFβ1 and activin. Indeed, one study estimated that Nodal is approximately 250 times less potent than activin A (48). The lower intrinsic activity of Nodal compared with other TGFβ ligands does not mean that it is less biologically relevant. In embryos, Nodal functions as a morphogen and not only acts where it is expressed, but also at a distance in a concentration-dependent manner (11). The concentrations of rNodal used on DU145 and LNCaP cells were lower than other studies with hESCs and pancreatic cells (12,15,49). It should also be noted that LNCaP and DU145 cells are heterozygous for single nucleotide deletions in the kinase domain of ActRIIA that diminish its ability to initiate downstream signaling (50). The intensity of Nodal signaling is also determined by the amount of cell surface or soluble Cripto-1. Although Cripto-1 is essential for Nodal activation of ActRIIA/B and Alk4/7, it reduces the potency and efficiency of the receptor complex (48). High levels of Cripto-1 also attenuate activin and TGFβ signaling, including in PC3 cells (37,51). Therefore, the relative levels of Nodal, activins, TGFβ, and Cripto-1 will all determine the amount of downstream Smad 2/3 phosphorylation in prostate cancer cells.

Nodal signaling has important functional consequences because it promotes the growth of prostate cancer cells in Matrigel and soft agar. This is consistent with previous data showing that Nodal enhances the clonogenicity and tumorigenicity of breast cancer, melanoma and glioma cell lines (17–19). Further studies should focus on whether Cripto-1 has additional Nodal-independent functions in prostate cancer, just as it does in other tumors. For example, Cripto-1 stimulates epithelial-to-mesenchymal transition and angiogenesis in breast cancer (52). In this case, Cripto-1 would be an attractive therapeutic target to block the actions of Nodal and other converging pathways.

The AR pathway is critical for the growth and survival of prostate cancer cells and often intersects other signaling cascades. Cross-talk between AR and the TGFβ superfamily is well recognized. BMPs inhibit AR activity through Smad1, which acts as a co-repressor in prostate cancer cells (53). There is also a direct interaction between Smad3 and AR, although there are conflicting data on whether this enhances or represses AR activity (54,55). Evidently, the downstream effects of this interaction are highly context-dependent, which might explain why androgen-regulated gene expression is stimulated by activin but inhibited by TGFβ1 (55–57). The results of this study show that Nodal antagonizes AR activity, but whether this is through the Smad3–AR interaction has not yet been established. Transient transfection of a pre-pro-Nodal construct attenuated the activity of a PSA luciferase construct in LNCaP cells and stable transfection down-regulated the expression of endogenous PSA, KLK2, TMPRSS2 and NKX3.1. Notably, previous studies have demonstrated that androgens reduce the clonogenicity of prostate cancer cells (58). Therefore, the decreased androgen responsiveness of LNCaP-Nodal cells is also consistent with their increased clonogenicity in soft agar assays shown in this study.

Given the similarities between cancer and development, the expression of Nodal in prostate cancer raises the question of whether it is also involved in prostate growth and morphogenesis. Tissue recombination experiments have shown that urogenital mesenchyme, the developmental precursor of prostatic stroma, can direct hESCs to differentiate into prostate ducts (59). The urogenital mesenchyme must support Nodal signaling in the early stages of this process because Nodal is required for specification of embryonic stem cells to definitive endoderm (60). It is also possible that Nodal influences later steps in prostate development. BMPs, TGFβ and activins all inhibit branching morphogenesis in the prostate (7). Yet in breast tissue, Nodal and Cripto-1 can stimulate ductal morphogenesis, unlike other the members of the TGFβ family (10). This suggests that Nodal may have a role in prostate development, but one that is different from other TGFβ ligands.

In summary, this study identifies the re-activation of Nodal as a novel pathway associated with the progression of prostate cancer and illustrates another example of the similarities between prostate cancer and development.

Acknowledgments

We gratefully acknowledge the staff at Sullivan Nicolaides Pathology for their assistance with immunohistochemistry, Prof Glenn Francis for the use of a digital slide scanner, and staff at the Australian Stem Cell Centre StemCore for providing hESC samples. We also thank members of the Australian Prostate Cancer Research Centre-Queensland and the Cancer Biology and Epigenomics Program at CMRC, especially Prof Luigi Strizzi, for their helpful advice. We are also grateful to the study participants, urologists, nurses and histopathologists for providing access to specimens for the TMAs, and Helen Hughes (Hanson Institute, Adelaide), Ruth Pe Benito (Garvan Institute, Sydney) and James Kench for technical contributions to the TMA construction.

Grant Support: This study was supported by funding from the Queensland Government Growing the Smart State PhD Program (MGL & JAC), Australian-American Fulbright Association (MGL), The Cancer Council Queensland (MGL), National Health and Medical Research Council (NHMRC) of Australia (#443234, JAC; #553045, DL), and National Institutes of Health (CA121205, MJCH)

References

1. Pierce GB, Speers WC. Tumors as caricatures of the process of tissue renewal: prospects for therapy by directing differentiation. Cancer Res. 1988; 48(8):1996–2004. [PubMed: 2450643]
2. Marker PC. Does prostate cancer co-opt the developmental program? Differentiation. 2008; 76(6): 736–744. [PubMed: 18752496]
3. Schaeffer EM, Marchionni L, Huang Z, Simons B, Blackman A, Yu W, Parmigiani G, Berman DM. Androgen-induced programs for prostate epithelial growth and invasion arise in embryogenesis and are reactivated in cancer. Oncogene. 2008; 27(57):7180–7191. [PubMed: 18794802]

4. Pritchard C, Mecham B, Dumpit R, Coleman I, Bhattacharjee M, Chen Q, Sikes RA, Nelson PS. Conserved gene expression programs integrate mammalian prostate development and tumorigenesis. Cancer Res. 2009; 69(5):1739–1747. [PubMed: 19223557]
5. Naxerova K, Bult CJ, Peaston A, Fancher K, Knowles BB, Kasif S, Kohane IS. Analysis of gene expression in a developmental context emphasizes distinct biological leitmotifs in human cancers. Genome Biol. 2008; 9(7):R108. [PubMed: 18611264]
6. Dhanasekaran SM, Dash A, Yu J, Maine IP, Laxman B, Tomlins SA, Creighton CJ, Menon A, Rubin MA, Chinnaiyan AM. Molecular profiling of human prostate tissues: insights into gene expression patterns of prostate development during puberty. FASEB J. 2005; 19(2):243–245. [PubMed: 15548588]
7. Prins GS, Putz O. Molecular signaling pathways that regulate prostate gland development. Differentiation. 2008; 76(6):641–659. [PubMed: 18462433]
8. Ao M, Franco OE, Park D, Raman D, Williams K, Hayward SW. Cross-talk between paracrine-acting cytokine and chemokine pathways promotes malignancy in benign human prostatic epithelium. Cancer Res. 2007; 67(9):4244–4253. [PubMed: 17483336]
9. Danielpour D. Functions and regulation of transforming growth factor-beta (TGF-beta) in the prostate. Eur J Cancer. 2005; 41(6):846–857. [PubMed: 15808954]
10. Kenney NJ, Adkins HB, Sanicola M. Nodal and Cripto-1: embryonic pattern formation genes involved in mammary gland development and tumorigenesis. J Mammary Gland Biol Neoplasia. 2004; 9(2):133–144. [PubMed: 15300009]
11. Schier AF. Nodal morphogens. Cold Spring Harb Perspect Biol. 2009; 1(5):a003459. [PubMed: 20066122]
12. Zhang YQ, Sterling L, Stotland A, Hua H, Kritzik M, Sarvetnick N. Nodal and lefty signaling regulates the growth of pancreatic cells. Dev Dyn. 2008; 237(5):1255–1267. [PubMed: 18393305]
13. Mesnard D, Guzman-Ayala M, Constam DB. Nodal specifies embryonic visceral endoderm and sustains pluripotent cells in the epiblast before overt axial patterning. Development. 2006; 133(13):2497–2505. [PubMed: 16728477]
14. James D, Levine AJ, Besser D, Hemmati-Brivanlou A. TGFbeta/activin/nodal signaling is necessary for the maintenance of pluripotency in human embryonic stem cells. Development. 2005; 132(6):1273–1282. [PubMed: 15703277]
15. Vallier L, Alexander M, Pedersen RA. Activin/Nodal and FGF pathways cooperate to maintain pluripotency of human embryonic stem cells. J Cell Sci. 2005; 118(Pt 19):4495–4509. [PubMed: 16179608]
16. Foley AC, Korol O, Timmer AM, Mercola M. Multiple functions of Cerberus cooperate to induce heart downstream of Nodal. Dev Biol. 2007; 303(1):57–65. [PubMed: 17123501]
17. Lee CC, Jan HJ, Lai JH, Ma HI, Hueng DY, Lee YC, Cheng YY, Liu LW, Wei HW, Lee HM. Nodal promotes growth and invasion in human gliomas. Oncogene. 2010; 29(21):3110–3123. [PubMed: 20383200]
18. Postovit LM, Margaryan NV, Seftor EA, Kirschmann DA, Lipavsky A, Wheaton WW, Abbott DE, Seftor RE, Hendrix MJC. Human embryonic stem cell microenvironment suppresses the tumorigenic phenotype of aggressive cancer cells. Proc Natl Acad Sci U S A. 2008; 105(11):4329–4334. [PubMed: 18334633]
19. Topczewska JM, Postovit LM, Margaryan NV, Sam A, Hess AR, Wheaton WW, Nickoloff BJ, Topczewski J, Hendrix MJC. Embryonic and tumorigenic pathways converge via Nodal signaling: role in melanoma aggressiveness. Nat Med. 2006; 12(8):925–932. [PubMed: 16892036]
20. Papageorgiou I, Nicholls PK, Wang F, Lackmann M, Makanji Y, Salamonsen LA, Robertson DM, Harrison CA. Expression of nodal signalling components in cycling human endometrium and in endometrial cancer. Reprod Biol Endocrinol. 2009; 7:122. [PubMed: 19874624]
21. Shen MM. Nodal signaling: developmental roles and regulation. Development. 2007; 134(6): 1023–1034. [PubMed: 17287255]
22. Reissmann E, Jornvall H, Blokzijl A, Andersson O, Chang C, Minchiotti G, Persico MG, Ibanez CF, Brivanlou AH. The orphan receptor ALK7 and the Activin receptor ALK4 mediate signaling by Nodal proteins during vertebrate development. Genes Dev. 2001; 15(15):2010–2022. [PubMed: 11485994]

23. Strizzi L, Bianco C, Normanno N, Salomon D. Cripto-1: a multifunctional modulator during embryogenesis and oncogenesis. Oncogene. 2005; 24(37):5731–5741. [PubMed: 16123806]
24. Luo J, Zha S, Gage WR, Dunn TA, Hicks JL, Bennett CJ, Ewing CM, Platz EA, Ferdinandusse S, Wanders RJ, Trent JM, Isaacs WB, De Marzo AM. Alpha-methylacyl-CoA racemase: a new molecular marker for prostate cancer. Cancer Res. 2002; 62(8):2220–2226. [PubMed: 11956072]
25. Lawrence MG, Lai J, Clements JA. Kallikreins on steroids: structure, function, and hormonal regulation of prostate-specific antigen and the extended kallikrein locus. Endocr Rev. 2010; 31(4): 407–446. [PubMed: 20103546]
26. Mostaghel EA, Page ST, Lin DW, Fazli L, Coleman IM, True LD, Knudsen B, Hess DL, Nelson CC, Matsumoto AM, Bremner WJ, Gleave ME, Nelson PS. Intraprostatic androgens and androgen-regulated gene expression persist after testosterone suppression: therapeutic implications for castration-resistant prostate cancer. Cancer Res. 2007; 67(10):5033–5041. [PubMed: 17510436]
27. Lai J, Myers SA, Lawrence MG, Odorico DM, Clements JA. Direct progesterone receptor and indirect androgen receptor interactions with the kallikrein-related peptidase 4 gene promoter in breast and prostate cancer. Mol Cancer Res. 2009; 7(1):129–141. [PubMed: 19147544]
28. Loessner D, Stok KS, Lutolf MP, Hutmacher DW, Clements JA, Rizzi SC. Bioengineered 3D platform to explore cell-ECM interactions and drug resistance of epithelial ovarian cancer cells. Biomaterials. 2010; 31(32):8494–8506. [PubMed: 20709389]
29. Lai J, Kedda MA, Hinze K, Smith RL, Yaxley J, Spurdle AB, Morris CP, Harris J, Clements JA. PSA/KLK3 AREI promoter polymorphism alters androgen receptor binding and is associated with prostate cancer susceptibility. Carcinogenesis. 2007; 28(5):1032–1039. [PubMed: 17151093]
30. Blanchet MH, Le Good JA, Mesnard D, Oorschot V, Baflast S, Minchiotti G, Klumperman J, Constam DB. Cripto recruits Furin and PACE4 and controls Nodal trafficking during proteolytic maturation. EMBO J. 2008; 27(19):2580–2591. [PubMed: 18772886]
31. Scognamiglio B, Baldassarre G, Cassano C, Tucci M, Montuori N, Dono R, Lembo G, Barra A, Lago CT, Viglietto G, Rocchi M, Persico MG. Assignment of human teratocarcinoma derived growth factor (TDGF) sequences to chromosomes 2q37, 3q22, 6p25 and 19q13.1. Cytogenet Cell Genet. 1999; 84(3–4):220–224. [PubMed: 10393436]
32. Saloman DS, Bianco C, Ebert AD, Khan NI, De Santis M, Normanno N, Wechselberger C, Seno M, Williams K, Sanicola M, Foley S, Gullick WJ, Persico G. The EGF-CFC family: novel epidermal growth factor-related proteins in development and cancer. Endocr Relat Cancer. 2000; 7(4):199–226. [PubMed: 11174844]
33. Yan YT, Liu JJ, Luo Y, EC, Haltiwanger RS, Abate-Shen C, Shen MM. Dual roles of Cripto as a ligand and coreceptor in the nodal signaling pathway. Mol Cell Biol. 2002; 22(13):4439–4449. [PubMed: 12052855]
34. Cocciadiferro L, Miceli V, Kang KS, Polito LM, Trosko JE, Carruba G. Profiling cancer stem cells in androgen-responsive and refractory human prostate tumor cell lines. Ann N Y Acad Sci. 2009; 1155:257–262. [PubMed: 19250213]
35. Shepherd CJ, Rizzo S, Ledaki I, Davies M, Brewer D, Attard G, de Bono J, Hudson DL. Expression profiling of CD133+ and CD133− epithelial cells from human prostate. Prostate. 2008; 68(9):1007–1024. [PubMed: 18398820]
36. Xing PX, Hu XF, Pietersz GA, Hosick HL, McKenzie IF. Cripto: a novel target for antibody-based cancer immunotherapy. Cancer Res. 2004; 64(11):4018–4023. [PubMed: 15173016]
37. Kelber JA, Panopoulos AD, Shani G, Booker EC, Belmonte JC, Vale WW, Gray PC. Blockade of Cripto binding to cell surface GRP78 inhibits oncogenic Cripto signaling via MAPK/PI3K and Smad2/3 pathways. Oncogene. 2009; 28(24):2324–2336. [PubMed: 19421146]
38. Sun C, Orozco O, Olson DL, Choi E, Garber E, Tizard R, Szak S, Sanicola M, Carulli JP. CRIPTO3, a presumed pseudogene, is expressed in cancer. Biochem Biophys Res Commun. 2008; 377(1):215–220. [PubMed: 18835250]
39. Lu S, Lee J, Revelo M, Wang X, Lu S, Dong Z. Smad3 is overexpressed in advanced human prostate cancer and necessary for progressive growth of prostate cancer cells in nude mice. Clin Cancer Res. 2007; 13(19):5692–5702. [PubMed: 17908958]

40. Yang S, Zhong C, Frenkel B, Reddi AH, Roy-Burman P. Diverse biological effect and Smad signaling of bone morphogenetic protein 7 in prostate tumor cells. Cancer Res. 2005; 65(13): 5769–5777. [PubMed: 15994952]
41. Strizzi L, Abbott DE, Salomon DS, Hendrix MJC. Potential for cripto-1 in defining stem cell-like characteristics in human malignant melanoma. Cell Cycle. 2008; 7(13):1931–1935. [PubMed: 18604175]
42. Bianco C, Strizzi L, Rehman A, Normanno N, Wechselberger C, Sun Y, Khan N, Hirota M, Adkins H, Williams K, Margolis RU, Sanicola M, Salomon DS. A Nodal- and ALK4-independent signaling pathway activated by Cripto-1 through Glypican-1 and c-Src. Cancer Res. 2003; 63(6): 1192–1197. [PubMed: 12649175]
43. Chu J, Ding J, Jeays-Ward K, Price SM, Placzek M, Shen MM. Non-cell-autonomous role for Cripto in axial midline formation during vertebrate embryogenesis. Development. 2005; 132(24): 5539–5551. [PubMed: 16291788]
44. Bianco C, Strizzi L, Mancino M, Rehman A, Hamada S, Watanabe K, De Luca A, Jones B, Balogh G, Russo J, Mailo D, Palaia R, D'Aiuto G, Botti G, Perrone F, Salomon DS, Normanno N. Identification of cripto-1 as a novel serologic marker for breast and colon cancer. Clin Cancer Res. 2006; 12(17):5158–5164. [PubMed: 16951234]
45. Shi Y, Massague J. Mechanisms of TGF-beta signaling from cell membrane to the nucleus. Cell. 2003; 113(6):685–700. [PubMed: 12809600]
46. Zhang Q, Rubenstein JN, Jang TL, Pins M, Javonovic B, Yang X, Kim SJ, Park I, Lee C. Insensitivity to transforming growth factor-beta results from promoter methylation of cognate receptors in human prostate cancer cells (LNCaP). Mol Endocrinol. 2005; 19(9):2390–2399. [PubMed: 15905358]
47. Zhao H, Shiina H, Greene KL, Li LC, Tanaka Y, Kishi H, Igawa M, Kane CJ, Carroll P, Dahiya R. CpG methylation at promoter site -140 inactivates TGFbeta2 receptor gene in prostate cancer. Cancer. 2005; 104(1):44–52. [PubMed: 15895377]
48. Kelber JA, Shani G, Booker EC, Vale WW, Gray PC. Cripto is a noncompetitive activin antagonist that forms analogous signaling complexes with activin and nodal. J Biol Chem. 2008; 283(8): 4490–4500. [PubMed: 18089557]
49. Kumar A, Novoselov V, Celeste AJ, Wolfman NM, ten Dijke P, Kuehn MR. Nodal signaling uses activin and transforming growth factor-beta receptor-regulated Smads. J Biol Chem. 2001; 276(1): 656–661. [PubMed: 11024047]
50. Rossi MR, Ionov Y, Bakin AV, Cowell JK. Truncating mutations in the ACVR2 gene attenuates activin signaling in prostate cancer cells. Cancer Genet Cytogenet. 2005; 163(2):123–129. [PubMed: 16337854]
51. Gray PC, Shani G, Aung K, Kelber J, Vale W. Cripto binds transforming growth factor beta (TGF-beta) and inhibits TGF-beta signaling. Mol Cell Biol. 2006; 26(24):9268–9278. [PubMed: 17030617]
52. Bianco C, Rangel MC, Castro NP, Nagaoka T, Rollman K, Gonzales M, Salomon DS. Role of Cripto-1 in stem cell maintenance and malignant progression. Am J Pathol. 2010; 177(2):532–540. [PubMed: 20616345]
53. Qiu T, Grizzle WE, Oelschlager DK, Shen X, Cao X. Control of prostate cell growth: BMP antagonizes androgen mitogenic activity with incorporation of MAPK signals in Smad1. EMBO J. 2007; 26(2):346–357. [PubMed: 17183365]
54. Kang HY, Huang KE, Chang SY, Ma WL, Lin WJ, Chang C. Differential modulation of androgen receptor-mediated transactivation by Smad3 and tumor suppressor Smad4. J Biol Chem. 2002; 277(46):43749–43756. [PubMed: 12226080]
55. Hayes SA, Zarnegar M, Sharma M, Yang F, Peehl DM, ten Dijke P, Sun Z. SMAD3 represses androgen receptor-mediated transcription. Cancer Res. 2001; 61(5):2112–2118. [PubMed: 11280774]
56. Fujii Y, Kawakami S, Okada Y, Kageyama Y, Kihara K. Regulation of prostate-specific antigen by activin A in prostate cancer LNCaP cells. Am J Physiol Endocrinol Metab. 2004; 286(6):E927–931. [PubMed: 14761877]

57. Gerdes MJ, Dang TD, Larsen M, Rowley DR. Transforming growth factor-beta1 induces nuclear to cytoplasmic distribution of androgen receptor and inhibits androgen response in prostate smooth muscle cells. Endocrinology. 1998; 139(8):3569–3577. [PubMed: 9681509]

58. Wolf DA, Schulz P, Fittler F. Synthetic androgens suppress the transformed phenotype in the human prostate carcinoma cell line LNCaP. Br J Cancer. 1991; 64(1):47–53. [PubMed: 1713053]

59. Taylor RA, Cowin PA, Cunha GR, Pera M, Trounson AO, Pedersen J, Risbridger GP. Formation of human prostate tissue from embryonic stem cells. Nat Methods. 2006; 3(3):179–181. [PubMed: 16489334]

60. Takenaga M, Fukumoto M, Hori Y. Regulated Nodal signaling promotes differentiation of the definitive endoderm and mesoderm from ES cells. J Cell Sci. 2007; 120(Pt 12):2078–2090. [PubMed: 17535850]

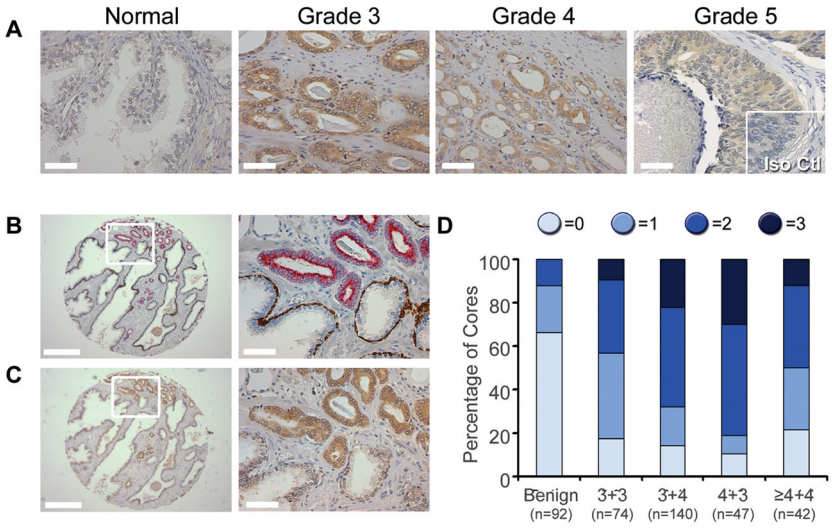

Figure 1. Nodal Expression in Prostate Tissues

(A) Representative images of Nodal immunohistochemistry (brown color) showing stronger staining in regions of Gleason pattern 3 to 5 cancer compared to normal glands. No immunoreactivity was observed with the isotype control antibody (Iso Ctl; Grade 5 inset). Scale bars, 50 μm. (B) Benign glands with p63- and high molecular weight cytokeratin-positive (brown staining) basal cells adjacent to AMACR-positive (red staining) malignant glands. (C) Stronger Nodal staining was apparent in malignant cells compared with benign glands. For B and C, scale bars for low magnification images on the left are 500 μm, and scale bars for high magnification images on the right are 50 μm. These are serial sections. (D) A graph comparing Nodal immunoreactivity, scored as no staining (0), weak (1), moderate (2) or strong (3), in cores of benign prostate and Gleason score 3+3, 3+4, 4+3 and ≥ 4+4 cancer. There was a significant correlation between Nodal staining and cancer versus benign cores (χ^2 test, $P=0.4\times10^{-21}$) as well as between high grade (Gleason scores 7 and higher) compared with low grade (Gleason score 6) prostate cancer (χ^2 test, $P=0.9\times10^{-4}$).

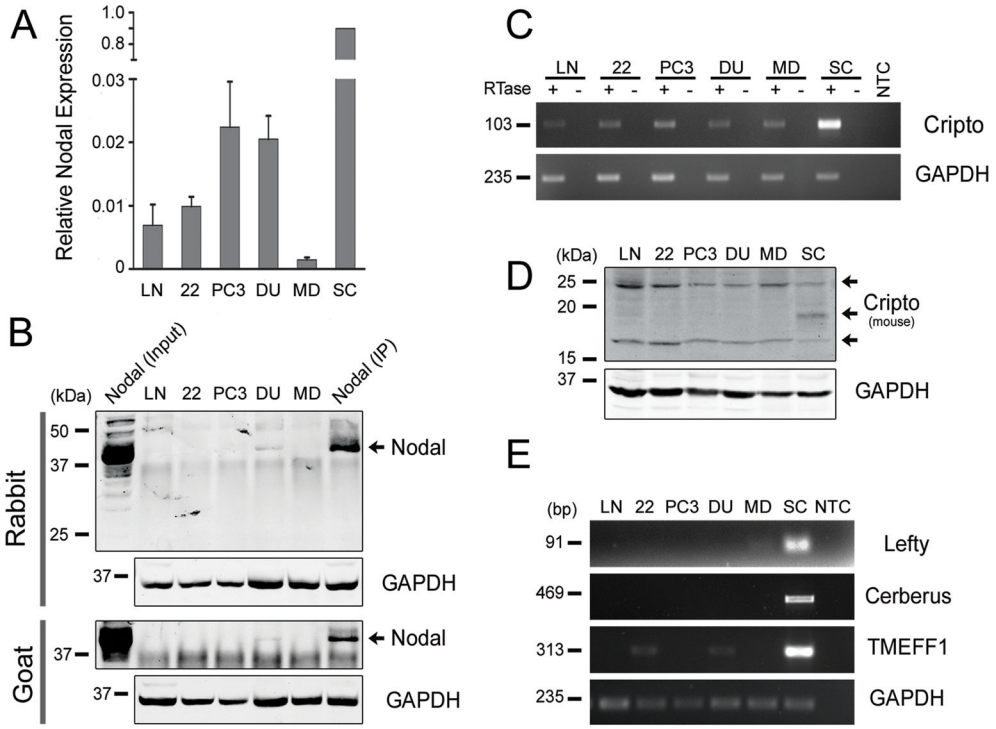

Figure 2. Nodal Expression in Prostate Cancer Cell Lines

(A) Real-time PCR of Nodal expression in prostate cancer cell lines normalized to H9 hESCs (n=3). (B) Western blots of lysates from prostate cancer cell lines immunoprecipitated using rabbit or goat anti-Nodal antibodies. LNCaP cells stably transfected with Nodal were used as a positive control for the Western blot (Nodal Input) and IP (Nodal IP). All blots were probed with a mouse anti-Nodal antibody. Nodal was detected as a single ~42 kDa band. The unbound fractions of IP samples were probed for GAPDH to compare initial protein concentrations. (C) RT-PCR showing that Cripto-1 was expressed in all prostate cell lines. H9 hESC was used as a positive control and GAPDH as the house-keeping gene. (D) Western blots of prostate cancer and MEL1 hESC lysates where Cripto-1 was detected as two bands of approximately 17 and 25 kDa. GAPDH was used as a loading control. (E) RT-PCR showing negligible Lefty and Cerberus expression in prostate cancer cells compared to H9 hESCs. Low levels of TMEFF1 were expressed in 22Rv1 and DU145 cells. LN = LNCaP, 22 = 22Rv1, DU = DU145, MD = MDAPCa2b, SC = H9 or MEL1 hESCs, RTase = reverse transcriptase, and NTC = no template control.

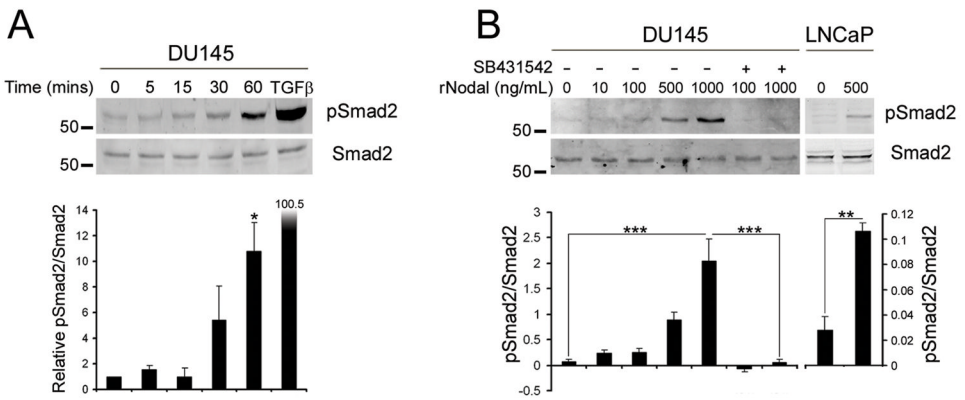

Figure 3. Nodal Signaling in Prostate Cancer Cell Lines

(A) DU145 cells were treated for 5–60 mins with 1 μg/mL recombinant Nodal or 30 min with 1 ng/mL TGFβ1. Western blots of pSmad2 and total Smad2 levels were quantified using densitometry. Nodal significantly increased Smad2 phosphorylation at 60 mins (One Way Anova with Tukey's posthoc analysis, n=2, **P*<0.05). (B) DU145 cells were treated for 60 min with 10–1000 ng/mL Nodal and 10 μM SB431542 (+) or DMSO control (−). LNCaP cells were treated with 500 ng/mL Nodal for 6 hrs with fresh Nodal added every 2 hrs. There was a significant increase in pSmad2 with 1 μg/mL Nodal in DU145 cells and significant decrease when SB431542 was added (One Way Anova with Tukey's posthoc analysis, n=3, ****P*<0.001). There was also a significant increase in Smad2 phosphorylation in LNCaP cells treated with Nodal (t test, n=3, ***P*<0.01).

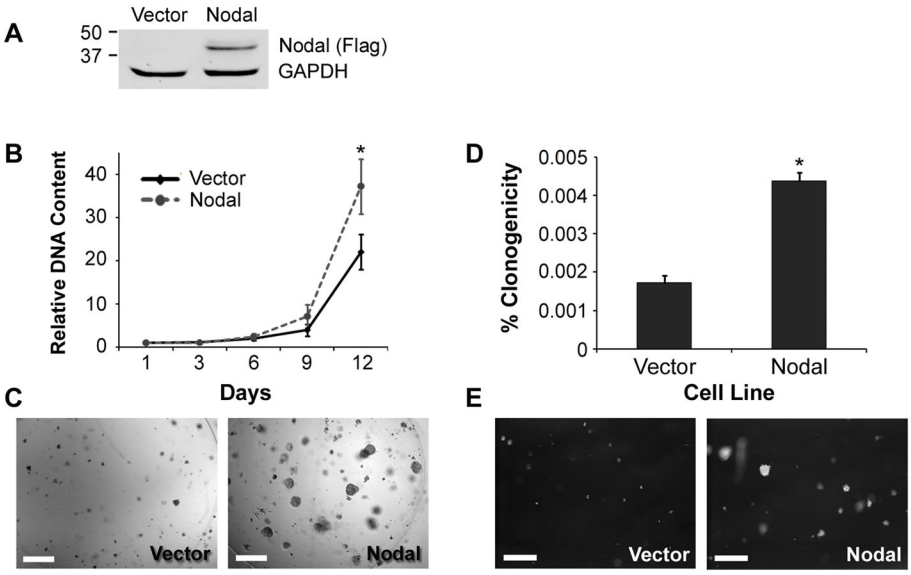

Figure 4. Nodal Increases the Growth of Prostate Cancer Cells

(A) A Western blot with a FLAG antibody confirming exogenous Nodal expression in LNCaP-Nodal, but not in LNCaP-Vector cells. The membrane was reprobed for GAPDH to verify equal loading. (B) The growth of LNCaP-Vector and LNCaP-Nodal cells in Matrigel constructs measured by DNA content after 1–12 days culture. Data are normalized to day 1. By day 12, there was a significant increase in the number of LNCaP-Nodal cells compared to the vector control (Two Way Anova with Tukey's posthoc analysis, n=3, $*P<0.05$). (C) Representative phase contrast images showing that LNCaP-Nodal cells formed larger clusters than LNCaP-Vector cells embedded within Matrigel constructs. Scale bars, 250 μm. (D) In soft agar assays, a significantly higher proportion of LNCaP-Nodal cells formed colonies compared with LNCaP-Vector cells (t test, n=3, $*P<0.05$). (E) Representative phase contrast images confirming that LNCaP-Nodal cells formed more prominent colonies. Scale bars, equal 500 μm.

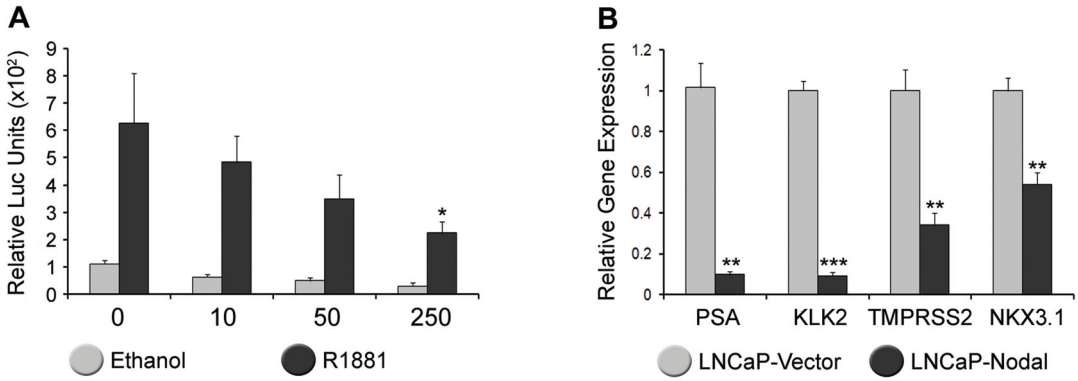

Figure 5. Nodal Antagonizes Androgen Receptor Signaling

(A) LNCaP cells transfected with 10–250 ng of Nodal and treated with 1 nM R1881. PSA luciferase activity relative to Renilla is significantly reduced by 250 ng of Nodal (Two way Anova with Tukey's posthoc analysis, n=3, $*P<0.05$). (B) Real-time PCR of PSA, KLK2, TMPRSS2, and NKX3.1 which were all significantly down-regulated in LNCaP cells stably transfected with Nodal compared with the vector control (t test, n=3, $**P<0.01$, $***P<0.001$).

Table 1

Primer sequences

Gene	Primer Sequences (5′ – 3′)	Reference
Cerberus	Fwd: CAAAGAGAGCTTCCCACAGG Rev: AATGAACAGACCCGCATTTC	-
Cripto-1	Fwd: AGAGATGACAGCATTTGGCCC Rev: AAAAGGACCCCAGCATGCA	-
GAPDH	Fwd: GCAAATTCCATGGCACCGT Rev: TCGCCCCACTTGATTTTGG	(25)
KLK2	Fwd: CTGCCCATTGCCTAAAGAAGAA Rev: GGCTTTGATGCTTCAGAAGGCT	(25)
Lefty A/B	Fwd: CTGCCGCCAGGAGATGTAC Rev: ACACTCATAAGCCAGGAAGCC	-
NKX3.1	Fwd: AACCATTTCACCCAGACAGCCT Rev: TGTGACAGATTGGAGCAGGGTT	(26)
PSA	Fwd: AGTGCGAGAAGCATTCCCAAC Rev: CCAGCAAGATCACGCTTTTGTT	(27)
TMEFF1	Fwd: TCTGCTCTTCGCCTTCTCTC Rev: GTGCTTACAAGCAGCCCTTC	-
TMPRSS2	Fwd: CCATTTGCAGGATCCGTCTG Rev: GGATGTGTCTTGGGGAGCAA	(26)